

Electrochemical, Kinetic, Antimicrobial (MIC) Studies of Acyclic Mononuclear Schiff-base Copper(II) Complexes

**A. Vijayaraj¹, R. Prabu¹, N. sivakumar³, R.Sangeetha Kumari⁴,
V. Kaviyaranan⁴, V.Narayanan^{2*}**

¹D.G. Vaishnav college (Autonomous) PG & Research Department of Chemistry, Arumbakkam Chennai- 600 106, India.

² Department of Inorganic Chemistry, School of Chemical Sciences, University of Madras, Guindy Maraimalai Campus, Chennai 600 025, India.

³Department of Chemistry, AMET University, Kanathur, Chennai 603 112

⁴Centre for Advanced Studies in Botany, University of Madras, Guindy Maraimalai Campus, Chennai 600 025, India.

Abstract : A series of mononuclear copper(II) complexes have been prepared by Schiff base condensation derived from 5-Bromosalicylaldehyde, diethylene triamine, tris(2-aminoethyl) amine, triethylene tetramine, N,N-bis(3-aminopropyl)ethylene diamine, N,N-bis(aminopropyl) piperazine and copper perchlorate. All the complexes were characterized by elemental and spectral analysis. Electronic spectra of the complexes show the d-d transition in the range of 575-620 nm, ESR spectra of the mononuclear copper(II) complexes show four lines, characteristic of square-planar geometry, with nuclear hyperfine spin 3/2. The copper(II) complexes show a normal room temperature magnetic moment value $\mu_{\text{eff}} = 1.71$ to 1.82 BM, which is close to the spin only value of 1.75 BM. Electrochemical studies of the complexes show irreversible one electron reduction process around -1.19 to -0.87 V. The reduction potential of the mononuclear copper(II) complexes shifts towards anodic direction upon increasing the chain length of the imine compartment. Electrochemical and catalytic studies of the complexes were compared on the basis of increasing the chain length of the imine compartment. All the complexes were screened for antifungal and antibacterial activity.

Keywords : Schiff-base ligands; copper(II) complexes; cyclic voltammetry; Catecholase activity.

Introduction

Schiff bases are important intermediates for the synthesis of some bioactive compounds¹. Furthermore; they are reported to show a variety of interesting biological actions, including antibacterial, antifungal, and anticancer. In the early days, the main efforts were directed towards synthesis and characterization of rather fundamental complexes, which do not look striking nowadays but were strongly needed in those days.

Schiff bases and their structural analogues, as ligating compounds containing acyclic and cyclic imine (C=N) bonds, are of great importance in modern coordination chemistry². Interest in metal complexes of these ligands is related to wide variability of their fine structures (rational design) and obtaining of polyfunctional materials³. Among them, we note luminescent complexes^{4,5} magnetoactive and liquid crystal structures⁶, chemosensors⁷ and other useful metal containing azomethine compounds. Bioinorganic and biomimetics are

widely represented⁸. Practically, all coordination compounds of Schiff bases were synthesized using chemical and electrochemical techniques. All factors forming mononuclear coordination compounds of Schiff bases are taken into account. Thereupon, a systematization of various types of Schiff-base complexes is offered.

The field of acyclic chemistry of metals is developing very rapidly because of its application^{9,10} and importance in the area of coordination chemistry¹¹. Studies on complexes of acyclic Schiff-base ligands with different size, and number and donor atoms for coordination with a variety of metal centers have been published¹². Many transition metal ions in living systems work as enzymes or carriers in a macrocyclic ligand environment. Meaningful research in this direction might generate simple models for biologically occurring metalloenzymes,^{13,14} and thus help in further understanding biological systems. The development of the field of bioinorganic chemistry has been another important factor in spurring the growth of interest in macrocyclic compounds^{15,16}. The stability of acyclic metal complexes depends upon a number of factors, including the number and types of donor atoms present in the ligand and their relative positions within the macrocyclic skeleton, as well as the number and size of the chelate rings formed on complexation. We reported recently Cu(II) Schiff base complexes in 2011.¹⁷ The present work deals with the influence of ligand modification on spectral, electrochemical, and kinetic studies, reporting the para-position variation of acyclic mononuclear copper (II) complexes.

Experimental

General procedures and materials

Elemental Analysis of the complexes is obtained using a Haereus CHN rapid analyzer. Conductivity measurement of the complexes is obtained using a Elico digital conductivity bridge modal CM-88 using freshly prepared solution of the complex in DMF. IR spectra were recorded on a PerkinElmer FT-IR 8300 series spectrophotometer on KBr disks from 4000 to 400 cm^{-1} . ^1H NMR spectra were recorded using a BRUKER GSX 300MHz NMR spectrometer. Mass spectra were obtained on a JEOL DX-303 mass spectrometer. Electronic spectral studies were carried out on a PerkinElmer 320 spectrophotometer from 200 to 1100 nm. Cyclic voltammograms were obtained on a CHI-600A electrochemical analyzer under oxygen-free conditions using a three-electrode cell in which a glassy carbon electrode was the working electrode, a saturated Ag/AgCl electrode was the reference electrode and platinum wire was the auxiliary electrode. A ferrocene/ferrocenium couple was used as an internal standard and $E_{1/2}$ of the ferrocene/ferrocenium (Fc/Fc^+) couple under the experimental condition was 470 mV. Tetra(n-butyl)ammonium perchlorate (TBAP) was used as the supporting electrolyte. Room temperature magnetic moments were measured on a PAR vibrating sample magnetometer Model- 155. X-band EPR spectra were recorded at 25 °C on a Varian EPR-E 112 spectrometer using diphenylpicrylhydrazine (DPPH) as the reference. Catalytic oxidation of catechol to o-quinone by the copper complexes was studied in 10^{-3} M dimethylformamide solutions. The reactions were followed spectrophotometrically with the strongest absorption band of o-quinone at 390 nm and monitoring the increase in absorbance. A plot of $\log (A_\infty/A_\infty - A_t)$ vs time was made for each complex and the rate constant for the catalytic oxidations were calculated.

Chemical and reagent

5-Bromosalicylaldehyde was prepared following the literature method. Analytical grade ethanol, acetonitrile, and DMF were purchased from Qualigens. TBAP, used as supporting electrolyte in electrochemical measurements, was purchased from Fluka and recrystallized from hot methanol. N,N-bis-(3-aminopropyl) piperazine, N,N-bis-(3-aminopropyl) ethylene diamine, and tris-(2-aminoethyl)amine were purchased from Aldrich. Triethylenetetramine and diethylenetriamine were purchased from Qualigens.

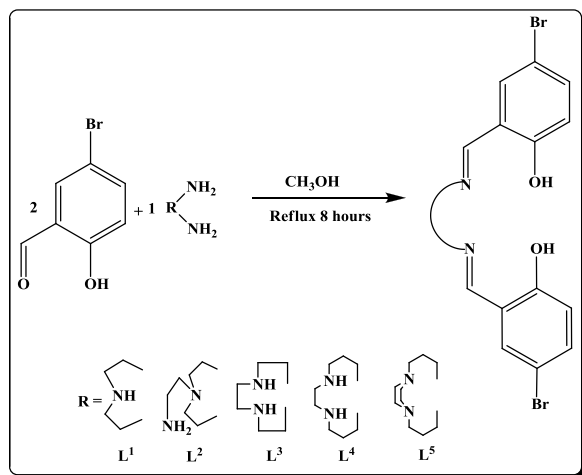
Synthesis of copper complexes

Synthesis of mono nuclear $[\text{Cu(II)}\text{L}^1(\text{ClO}_4)]$ Complex

An absolute methanol solution containing $\text{Cu}(\text{ClO}_4)_2 \cdot 6\text{H}_2\text{O}$ (0.0370 g, 0.1mmol) was added drop-wise to a stirring solution of L^1 (0.0466 g, 0.1mmol) in 20 mL of absolute methanol. The solution was refluxed for 8 hours the above reaction shown in Scheme 2. On cooling the solution yellow colour microcrystals are formed, which were filtered and washed with methanol followed by diethyl ether and dried in vacuum. The crude

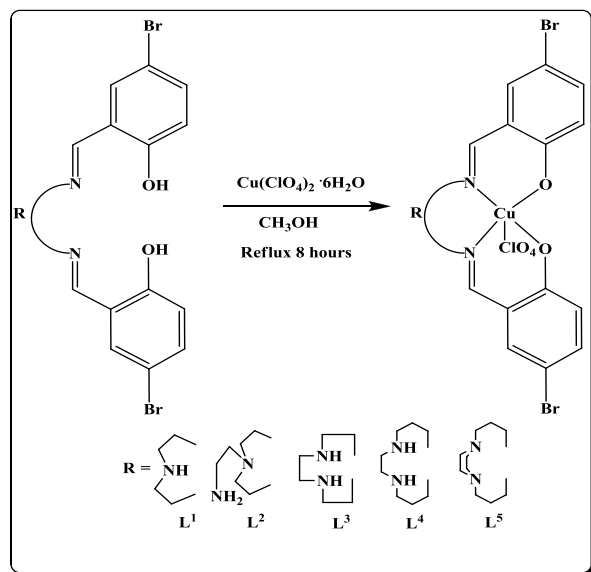
product was recrystallized from methanol and acetonitrile (1:3, v/v). $[\text{Cu(II)}\text{L}^2]$, $[\text{Cu(II)}\text{L}^3]$, $[\text{Cu(II)}\text{L}^4]$ and $[\text{Cu(II)}\text{L}^5]$ were synthesis by following the above procedure using L^2 (0.0512 g, 0.1mmol), L^3 (0.0512 g, 0.1mmol), L^4 (0.0540 g, 0.1mmol) and L^5 (0.0566 g, 0.1mmol) ligands.

Scheme-1



Scheme 1 Schematic diagram for the synthesis of ligands

Scheme-2



Scheme 2 Schematic diagram for the synthesis of Cu(II) complexes

Yield : (59%) m.p.: 321 °C (dec). Anal. for $\text{C}_{18}\text{H}_{16}\text{Br}_2\text{ClN}_3\text{O}_6\text{Cu}$; Calcd (%): C, 34.36; H, 2.56; N, 6.68; Cu, 10.10; Found (%): C, 34.35; H, 2.55; N, 6.69; Cu, 10.7; ESI Mass: (m/z 630.00 Calcd av. m/z 629.14). Conductance ($\Lambda \text{ Scm}^2 \text{ mol}^{-1}$) in DMF: 128. Selected IR data (KBr) (ν , cm^{-1}): 3123 b [ν (N-CH₂)], 1631 s [ν (C=N)], 1060 w [ν (ClO₄⁻) coordinated], 573 s [ν (M-N)], 467 s [ν (M-O)],

Synthesis of $[\text{Cu(II)}\text{L}^2]$ Complex

Yield : (56%) m.p.: 291 °C (dec). Anal. for $\text{C}_{20}\text{H}_{21}\text{Br}_2\text{N}_4\text{O}_2\text{Cu}$; Calcd (%): C, 41.94; H, 3.70; N, 9.78; Cu, 11.09; Found (%): C, 41.93; H, 3.71; N, 9.77; Cu, 11.07; ESI Mass: (m/z 573.13 Calcd av. m/z 572.76). Conductance ($\Lambda \text{ Scm}^2 \text{ mol}^{-1}$) in DMF: 53. Selected IR data (KBr) (ν , cm^{-1}): 3113 v (N-CH₂), 1634 [s, ν (C=N)], 583 [s, ν (M-N)], 475 [s, ν (M-O)].

Synthesis of [Cu(II)L³] Complex

Yield : (52%) m.p.: 225 °C (dec). Anal. for C₂₀H₂₀Br₂N₄O₂Cu; Calcd (%): C, 42.01; H, 3.53; N, 9.80; Cu, 11.11; Found (%):C, 41.98; H, 3.52; N, 9.78; Cu, 11.09; ESI Mass: (m/z 569.90 Calcd av. m/z 571.75). Conductance (Λ Scm² mol⁻¹) in DMF: 51. Selected IR data (KBr) (ν , cm⁻¹): 3123 ν (N-CH₂), 1627 [s, ν (C=N)], 573 [s, ν (M-N)], 469 [s, ν (M-O)].

Synthesis of [Cu(II)L⁴] Complex

Yield : (52%) m.p.: 224 °C (dec). Anal. for C₂₂H₂₄Br₂N₄O₂Cu; Calcd (%): C, 44.05; H, 4.03; N, 9.34; Cu, 10.59; Found (%):C, 44.02; H, 4.01; N, 9.33; Cu, 10.57; ESI Mass: (m/z 600.93 Calcd av. m/z 599.80). Conductance (Λ Scm² mol⁻¹) in DMF: 52. Selected IR data (KBr) (ν , cm⁻¹): 3125 ν (N-CH₂), 1622 [s, ν (C=N)], 562 [s, ν (M-N)], 464 [s, ν (M-O)].

Synthesis of [Cu(II)L⁵] Complex

Yield : (52%) m.p.: 225 °C (dec). Anal. For C₂₄H₂₈Br₂N₄O₂Cu; Calcd (%): C, 45.91; H, 4.50; N, 8.92; Cu, 10.12; Found (%): C, 45.89; H, 4.49; N, 8.91; Cu, 10.10; ESI Mass: (m/z 628.13 Calcd av. m/z 627.85). Conductance (Λ Scm² mol⁻¹) in DMF: 57. Selected IR data (KBr) (ν , cm⁻¹): 3110 ν (N-CH₂), 1629 [s, ν (C=N)], 571 [s, ν (M-N)], 476 [s, ν (M-O)].

Results and discussion

FT IR spectral analysis

The FT IR spectrum of the precursor compound (PC) shows a sharp band at around 1668 cm⁻¹ due to the presence of CHO group. The OH group in the ligand shows a broad peak at 3378 cm⁻¹. All the ligands show a band at 3389 cm⁻¹ due to the phenolic and aliphatic OH groups. The band in the region of 1636 - 1590 cm⁻¹ in the ligands is due to the presence of imine (C=N) group. All the complexes show a sharp band in the region 1636 - 1620 cm⁻¹, due to ν C=N stretching. The complete disappearance of aldehydic group of the precursor and the appearance of imine (CH=N-) group in the ligands show the effective Schiff base condensation between the aldehyde group of the precursor compound and the amine groups. For the complexes, bands at 460–490 cm⁻¹ could be assigned to -(M–O) bond. Other weak bands at lower frequency could be assigned to -(M–N) bond [19]. The spectra of all the complexes are dominated by bands at 3150-3070 cm⁻¹ due to the aromatic C-H stretching vibration. A strong band at 1260 cm⁻¹ in the free Schiff bases has been assigned to phenolic C–O stretching vibration. Upon complexation, this band shifts to higher frequency (1300 cm⁻¹) showing coordination through phenolic oxygen. The presence of uncoordinated perchlorate anions in all of the mononuclear complexes are inferred from a single broad band around 1100 cm⁻¹ (ν_3 -antisymmetric stretching) which are not split and a band around 650 cm⁻¹ (ν_4 -antisymmetric bending). The band around 930 cm⁻¹ (ν_2 - symmetric stretching) due to coordinated perchlorate, is not observed and this indicates that no perchlorate ions are coordinated in the complexes.

ESI Mass Spectral analysis

The ESI mass spectra of mono nuclear complexes [Cu(II)L¹], [Cu(II)L²], [Cu(II)L⁴], and [Cu(II)L⁵] the molecular ion peak (M⁺) at m/z = 630.00, 573.13, 600.93 and 628.13 respectively. The spectra show some prominent peaks corresponding to the various fragments of the complexes. The ESI mass spectra of mononuclear complexes [Cu(II)L²], shown in Figures 1.

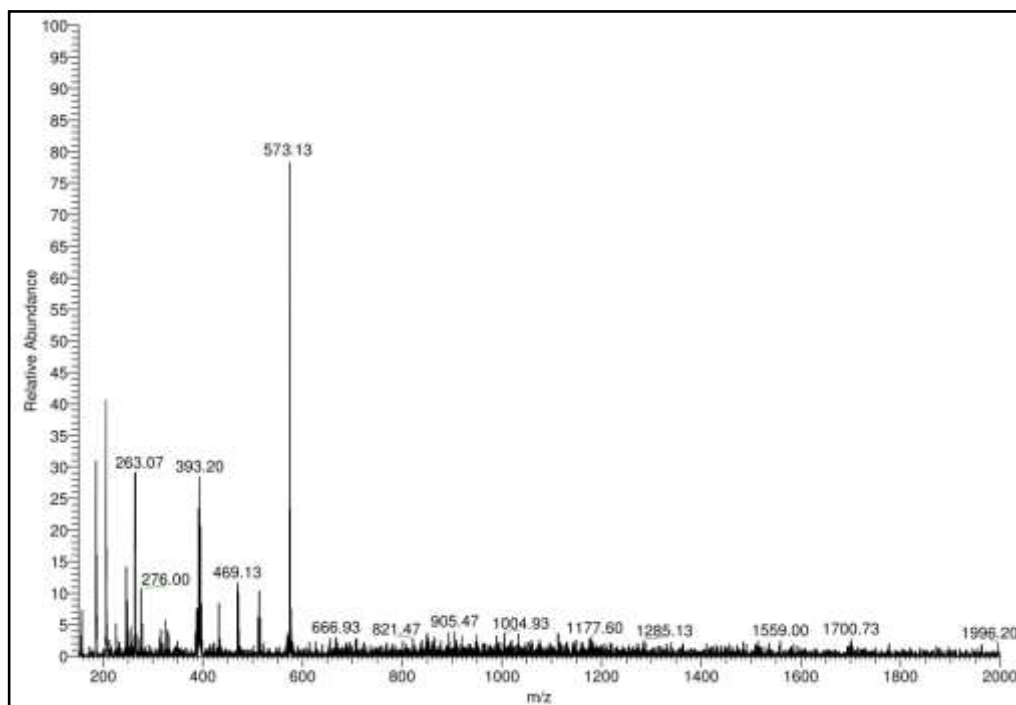


Figure 1. ESI Mass spectrum of $[\text{Cu(II)L}^2]$ complex m/z 573.13 $[\text{MH}^+]$

Electronic spectra

Electronic spectra of all the complexes were obtained in DMF medium. The electronic absorption spectra of Cu(II) complexes are recorded at 25 °C and the absorption region assignment data are given in Table 1 and the proposed geometry of the complexes are given. The electronic spectra of $[\text{Cu(II)L}^1]$ to $[\text{Cu(II)L}^5]$ complexes show a single weak d-d band in region 563-632 nm due to $d_{x^2-y^2} \rightarrow d_{xy}, d_{yz}, d_z^2, d_{xy}$ associated with distorted octahedral geometry around the $[\text{Cu(II)L}]$ ion. This red shift may be due to the distortion from planar geometry as the chain length increases. Moderately intense band observed in the region of 365-387 nm is associated with ligand to metal charge transfer transition. An intense band observed in the region 255-295 nm is associated with intra ligand transition. The electronic absorption spectra are given in Figures 2 to 3.

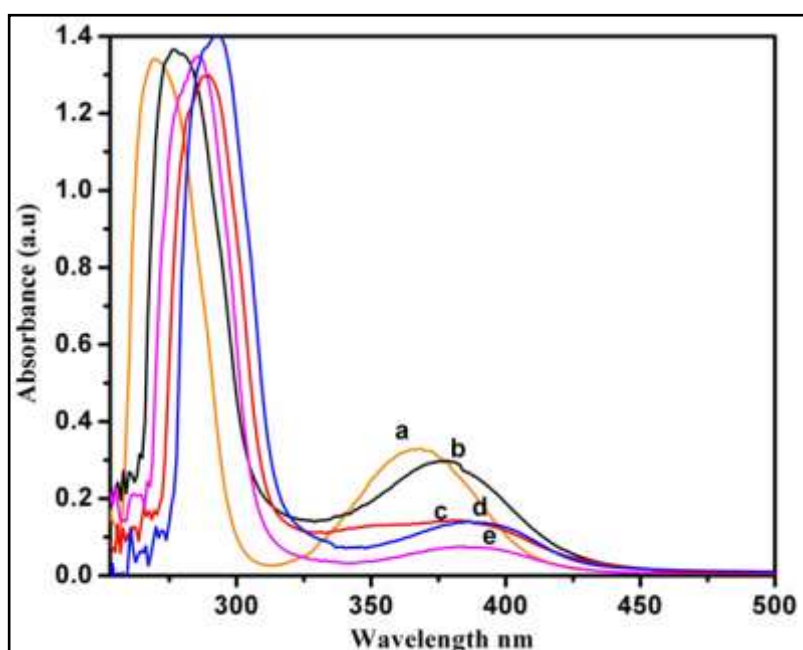


Figure 2. UV spectrum of mononuclear $[\text{Cu(II)L}^{1-5}]$ complexes

(a)[Cu(II)L¹(ClO₄)],(b)[Cu(II)L²],(c)[Cu(II)L³],(d)[Cu(II)L⁴] and (e)[Cu(II)L⁵]

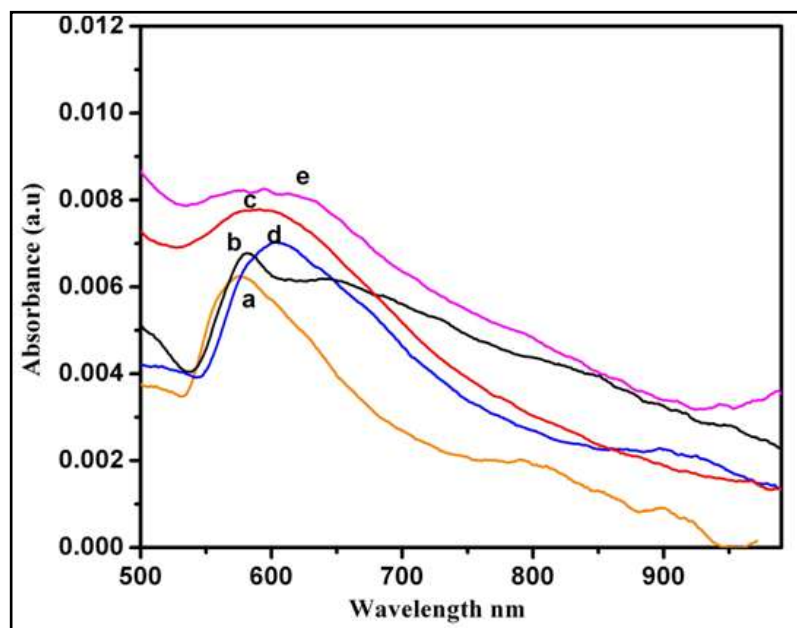


Figure 3. UV-Vis spectrum of mononuclear [Cu(II)L¹⁻⁵] complexes
(a)[Cu(II)L¹(ClO₄)],(b)[Cu(II)L²],(c)[Cu(II)L³],(d)[Cu(II)L⁴] and (e)[Cu(II)L⁵]

ESR spectra

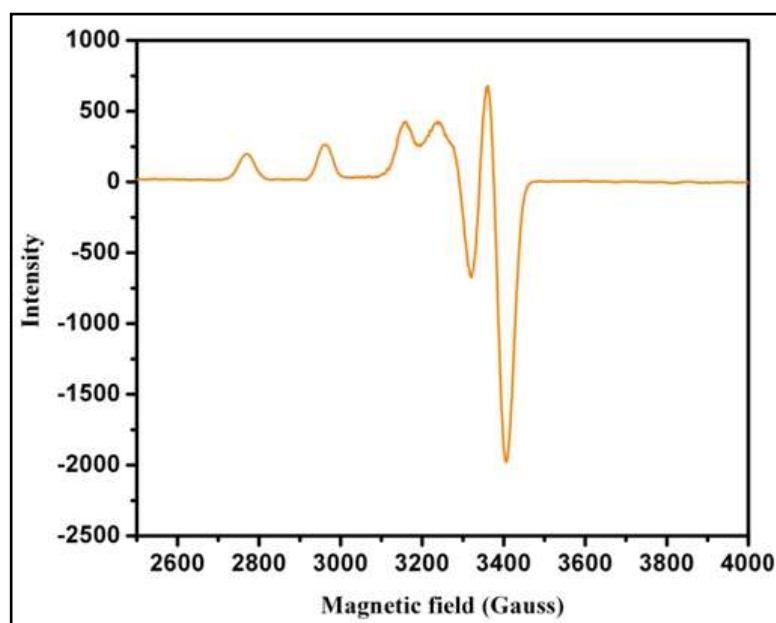


Figure 4. ESR spectrum of [Cu(II)L¹(ClO₄)] complex

ESR spectra of the copper(II) complexes recorded in the X-band region at room temperature, provides useful information which is important in studying the metal ion environment. The room temperature spectrum shows one intense absorption band in the high field region and it is isotropic, due to the tumbling motion of the molecule. The ESR spectra of [Cu(II)L] complexes show four lines due to hyperfine splitting (nuclear spin 3/2). ESR spectrum of [Cu(II)L¹] is given in Figure 4. The observed *g* values are less than 2.3 indicating considerable covalent character in the M–L bonds. The ESR data of [Cu(II)L¹⁻⁵] complexes are given in Table 2. *g*_{||} values of [Cu(II)L¹] 2.28, [Cu(II)L²] 2.29, [Cu(II)L³] 2.36, [Cu(II)L⁴] 2.25 and [Cu(II)L⁵] 2.17 and *g*_⊥ values are 2.09,

2.11, 2.12, 2.17 and 2.16 respectively, indicating square-planar geometry. The absence of the half-field signal at 1600 G, corresponding to $DM = \pm 2$ transition, ruled out Cu–Cu interaction [23], consistent with mononuclear complexes. The hyperfine A_{\parallel} splitting falls in the range of $150\text{--}165 \times 10^{-4} \text{ cm}^{-1}$, indicative of an electron interacting with only one copper nucleus. The relation $g_{\parallel} > g_{\perp}$ is typical of d^9 copper(II) complexes in a ground state doublet with the unpaired electron in a dx^2-y^2 orbital. The order $g_{\parallel} > g_{\perp} > 2$ and the ESR parameters coincide with related systems suggesting the square-planar geometry.

The room temperature (at 298 K) magnetic moments of the copper complexes were determined by vibrating sample magnetometer (VSM). The magnetic moments of copper(II) complexes are in the range of 1.71 to 1.77 BM, close to the spin-only value of copper(II) [25]. The room temperature magnetic data of the copper(II) complexes do not provide conclusive evidence for the geometry however the electronic spectral data coupled with magnetic moment values indicate the square planar geometry for all the copper(II) complexes.

Electrochemistry

Electrochemistry of copper complex (Reduction process at negative potential)

The electrochemical properties of the mononuclear complexes were studied by cyclic voltammetry in DMF solution containing TBAP as supporting electrolyte in the potential range to 0.0 to -1.60 V. The electrochemical data of $[\text{Cu(II)L}^{1-5}]$ complexes are given in Table 3a. The cyclic voltammogram is given in Figure 5. Generally the electrochemical properties of the complexes depend on a number of factors such as chelate ring/size axial ligation degree and distribution of unsaturation and substitution pattern in the chelate ring. Each voltammogram shows one electron irreversible reduction wave at a negative potential. The controlled potential electrolysis carried out at 100 mV more negative than the reduction wave conveys the consumption of one electron per molecule. It is very interesting to compare the electrochemical behavior of $[\text{Cu(II)L}]$ complexes. The reduction potential shift towards anodic direction for the complexes $[\text{Cu(II)L}^1]$ to $[\text{Cu(II)L}^5]$ from -1.19 V to -0.87 V, as the number of methylene groups between the imine nitrogen (chain length) increases. The entire acyclic ring became more flexible, which cause a distortion of the geometry of the copper(II) complexes and makes the system is more flexible, which stabilized the low valent Cu(I).

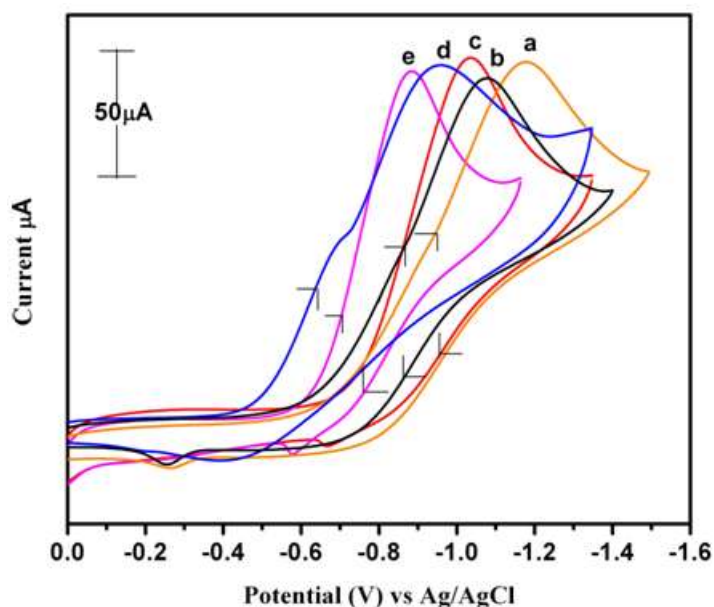


Figure 5. Cyclicvoltammograms of the mononuclear $[\text{Cu(II)L}^{1-5}]$ complexes:
(Reduction process) (a) $[\text{Cu(II)L}^1(\text{ClO}_4)]$, (b) $[\text{Cu(II)L}^2]$, (c) $[\text{Cu(II)L}^3]$, (d) $[\text{Cu(II)L}^4]$ and(e) $[\text{Cu(II)L}^5]$.

Kinetic Studies

Oxidation of Pyrocatechol (Catecholase Activity)

The catecholase activity of the copper(II) complexes synthesized in the present work was carried out using pyrocatechol as the convenient model substrate for the identification of functional models for the metalloenzymes [27]. For this purpose, 10^{-3} mol dm $^{-3}$ solutions of complexes in dimethylformamide were treated with 100 equivalents of pyrocatechol in the presence of air. The course of the reaction was followed spectrophotometrically at 390 nm for nearly 45 min at regular time intervals of 5 min. The slope was determined by the method of initial rates by monitoring the growth of the 390 nm band of the product o-quinone. A linear relationship for initial rate and the complex concentration obtained for both the copper(II) complexes shows a first-order dependence on the complex concentration for the systems.

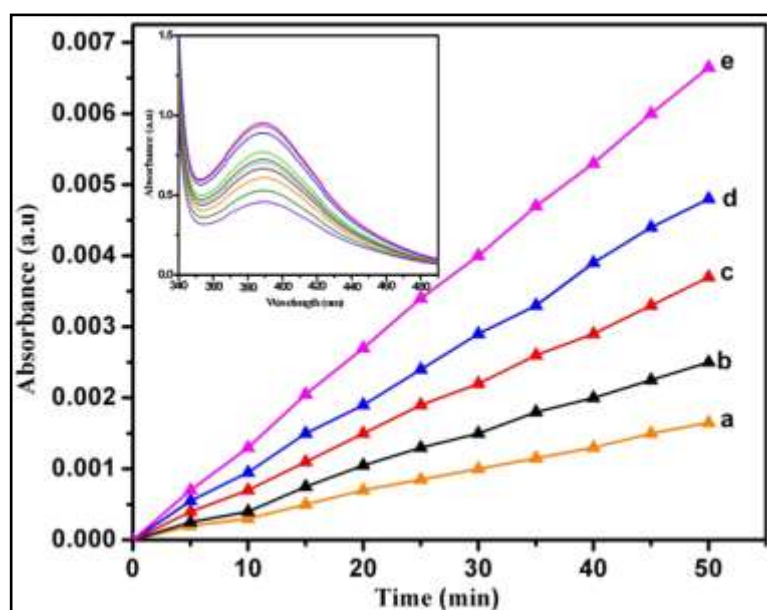
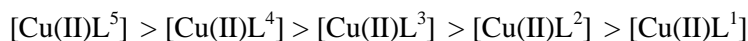


Figure 6. Catecholase activity of the $[\text{Cu(II)L}^{1-5}]$ complexes (a) $[\text{Cu(II)L}^1(\text{ClO}_4)]$, (b) $[\text{Cu(II)L}^2]$, (c) $[\text{Cu(II)L}^3]$, (d) $[\text{Cu(II)L}^4]$ and (e) $[\text{Cu(II)L}^5]$. The inset is the time dependent growth of the o-quinone chromophore in the presence of $[\text{Cu(II)L}^3]$

Plots of $\log (A_\infty/A_\infty - A_t)$ vs time for catecholase activity of the copper(II) complexes are obtained and shown in Figure 6. The inset in Figure 6 shows the time dependent growth of o-quinone chromophore in the presence of $[\text{Cu(II)L}^5]$. The observed initial rate constant value for copper(II) complexes is given in Table. 3b. The complex $[\text{Cu(II)L}^5]$ has higher catalytic activity ($3.68 \times 10^{-3} \text{ min}^{-1}$) than the complex $[\text{Cu(II)L}^4]$ ($2.66 \times 10^{-3} \text{ min}^{-1}$) which in turn is higher than the copper(II) complex $[\text{Cu(II)L}^1]$ ($0.91 \times 10^{-3} \text{ min}^{-1}$). The order of activity of the complexes is shown below.



From the results it is observed that the rate of oxidation of catecholase to o-quinone has increased as the chain length increases. The catecholase activity of complex containing longer carbon chain in the imine compartment is higher than that of the complex containing lesser carbon chain in the imine compartment, which is due to flexibility resulting from distortion of the coordination sphere. Increase in the chain length causes a greater distortion of the geometry of the complexes. This geometry may favour the observed higher rate of the reaction.

Conclusion

In conclusion, five Schiff base copper(II) complexes have been synthesized and their coordination chemistry. The electronic spectra of $[\text{Cu(II)L}^{1-5}]$ complexes indicates square planar geometry, and there is a red shift due to the increase in the chain length. Cyclic voltammograms exhibit one electron quasi-reversible

process. The reduction potential shifts to more negative potential on increasing chain length and oxidation potential shifts more positive potential on increasing chain length. All the $[\text{Cu(II)L}^{1-5}]$ complexes show good catalytic activity on increasing the chain length. Increase in the chain length causes a greater distortion of the geometry of the complexes. This flexibility in the geometry may favour the observed higher rate of the reaction.

Acknowledgements

Financial support from CSIR, New Delhi is gratefully acknowledged

References

1. Taggi A.E., Hafez A.M., Wack H., Young B., Ferraris D., Lectka T., The Development of the First Catalyzed Reaction of Ketenes and Imines: Catalytic, Asymmetric Synthesis of β -Lactams, Journal of American Chemistry. Society, 2002, 124, 6626-6635.
2. N. Raman, C. T. Thangaraja, S. Johnsonraja, N,N-dimethylbiguanide complexes displaying low cytotoxicity as potential large spectrum antimicrobial agents, European Journal of Medicinal Chemistry. 2005, 3, 537-345.
3. Mueller K., Schert U., Organic Light Emitting Devices Wiley-WCH Weinheim–New York, 2006.
4. Metelitsa A.V., Burlov A.S, Bezugly S.O., Borodkina I. G, Bren V.A., Garnovskii A.D., Synthetic Coordination and Organometallic Chemistry, Russian journal of coordination Chemistry, 2006, 32, 858-865.
5. Gatteschi D., Sessoli R., Cornia A., In Comprehensive Coordination Chemistry II, A.B.P. Lever, Elsevier-Pergamon Press, Amsterdam–Oxford–New York 2003.
6. Gunasekar V. Reshma K.R. Treesa G. Gowdhaman D. and Ponnusami V., Xanthan from sulphuric acid treated tapioca pulp : Influence of acid concentration on xanthan fermentation, Carbohydr. Polym.,2014, 102, 669–673.
7. J. C. Callan, A. P. Da-Silva, D. C. Magir., Cobalt(II), Nickel(II), Copper(II) and Zinc(II) complexes with new tetraaza schiff base ligands: Synthesis, characterization and thermodynamic studies Tetrahedron., 2005, 61, 8551 .
8. Holm R. H., Solomon E. I., Biomimetic Inorganic Chemistry, Chemical Review.,2004 104, 347-348.
9. Chaudhary A., Bansal N., Gajraj A., Singh R.V., Stereochemical and biochemical aspects of some organoboron complexes of sulphur donor Journal of Inorganic Biochemistry., 2003, 96, 393-400.
10. Wang Y. Tong X. Yan Y. Xue S. and Zhang Y., Efficient and selective conversion of hexose to 5-hydroxymethylfurfural with tin – zirconium-containing heterogeneous catalysts, Catal. Commun. 2014, 50, 38–43.
11. Benny I.S. Gunasekar V. and Ponnusami V., Review on Application of Xanthan Gum in DrugDelivery, International Journal of ChemTech Research, 2014, 6, 1322–1326.
12. Amado A.M., Ribeiro P.J.A., ClaroCoordination properties of 2-aminocyclopentene-1-dithiocarboxylic acid to transition metal ions as studied by initio calculations, journal of Inorganic Biochemistry., 2004, 98, 561.
13. Kumar A. and Ahuja M., Carboxymethyl gum kondagogu : Synthesis, characterization and evaluation as mucoadhesive polymer, Carbohydr. Polym., 2012, 90, 637–643.
14. Flayyih Ali S.T. Ghanim H.T., Synthesis and characterization of heterocyclic compounds from amine derivative, International Journal of ChemTech Research, 2016, 9, 360-367.
15. Saadon Abdulla Aowda.Synthesis and study of antioxidant activity of some Schiff's bases containing 1,2,3-triazole rings. International Journal of ChemTech Research.,2015,6, 659-664.
16. Ahmad. H, Moustapha F,K.C. Synthesis, Characterization, Biological Evaluation and Antibacterial Activity of some Heterocyclic Fluorene Compounds Derived from Schiff Base. International Journal of ChemTech Research.,2015, 8(2),447-458.
17. Kalpana V.N., Chakraborty P., Palanichamy V., Rajeswari V., Synthesis and characterization of copper nanoparticles using Tridax procumbens and its application in degradation of bismarck brown, 2016,9, 498-507.
